Imaging findings and differential diagnosis of hepatic sinusoidal occlusion syndrome and Budd-Chiari syndrome

Cui yu Jia (jiacuiyu@ccmu.edu.cn)
Beijing YouAn Hospital, Capital Medical University
Da wei Zhao (zhaoDW8999@163.com)
Beijing YouAn Hospital, Capital Medical University
Ji liang Feng
Beijing YouAn Hospital, Capital Medical University
Rui li Li
Beijing YouAn Hospital, Capital Medical University
Xin xin Wang
Beijing YouAn Hospital, Capital Medical University
Hong jun Li (lihongjun00113@ccmu.edu.cn)
Beijing YouAn Hospital, Capital Medical University

Research Article

Keywords: liver, Sinusoidal obstruction syndrome, Budd-Chiari syndrome, Computed tomography, Magnetic resonance imaging

Posted Date: March 17th, 2021

DOI: https://doi.org/10.21203/rs.3.rs-257653/v1

Abstract

Objective

To retrospectively analyze the clinical and imaging manifestations differential points between hepatic sinusoidal obstruction syndrome (SOS) and Budd-Chiari syndrome (BCS).

Material

The clinical symptoms, laboratory examination and imaging findings of 15 cases of hepatic sinusoidal obstruction syndrome and 33 cases of Budd-Chiari syndrome were statistically analyzed, find the identification points. The study used the Fisher test, P values of 0.05 or less were considered to indicate significant differences. The retrospective study was approved by the hospital's ethics committee.

Results

Laboratory tests: There were significant differences in total protein reduction rate (66.7% vs 9.1%, p□0.01), albumin reduction rate (66.7% vs 9.1%, p□0.01), Gamma-glutamyltransferase elevation rate (100% vs 6.1%, P□0.01), alkaline phosphatase elevation rate (60% vs 6.1%, p□0.01), and abnormal rate of prothrombin time (100% vs 21.2%, p□0.01) between the two groups (BCS vs SOS). It also indicates that the liver function of SOS patients is more seriously impaired. Image findings: The following image findings were observed significant more frequently in SOS than in BCS and were statistically significant: gallbladder wall thickening (66.7% vs 78.2%, p□0.01), ascites (80% vs 27.3%, p□0.01), cloverleaf or claw-like shapes (80% vs 0%, p□0.01). The following images appeared more frequently in BCS than in BCS and were statistically significant: caudate lobe enlargement (33.3% vs 75.8%, p□0.01), collateral circulation (46.7% vs 93.9%, p□0.01), diffuse patchy enhancement (20% vs 93.9%, p□0.01), homogeneous in delayed phase (13.3% vs 90.1%, p□0.01).

Conclusion

To Identification of SOS and BCS should be based on the patient's laboratory examination and imaging findings to improve diagnostic accuracy.

Introduction

Sinusoidal obstruction syndrome, also known as veno-occlusive disease (SOS), is a potentially life-threatening complication after hematopoietic stem cell transplantation (HCT). The severity of SOS varies widely, mild cases go into remission within a few weeks, while severe cases develop multiple organ failure, the mortality rate was as high as 84.3%[1, 2]. SOS is commonly seen in HCT in western countries

and is mainly caused by herb, such as Gynura segetum in China and some other Asian countries[3–6]. The imaging features of hemodynamic changes, liver parenchymal heterogeneity, liver function damage and portal hypertension provide important information for SOS diagnosis[7–9]. However, SOS and Budd-Chiari syndrome (BCS) often share similar clinical manifestations, such as hepatomegaly, hepatic distention pain, jaundice, ascites, and weight gain, which have always been the difficulties in clinical differentiation. The purpose of this paper is to investigate the clinical, imaging and pathological features of SOS and BCS, and to provide useful help for their differentiation.

Patients And Methods

This retrospective study has been approved by the ethics Committee of our hospital. There were 15 consecutive SOS pathologically diagnosed by biopsy at our institution from January, 2013 to October June, 2020. The following were the inclusion criteria: (a) patients who underwent contrast-enhanced dynamic CT and/or MR imaging within 2 weeks before biopsy; (b) all SOS cases were confirmed by histopathology in our hospital; (c) all the BCS cases had complete contrast-enhanced dynamic CT and/or MR imaging, DSA, among which 15 cases underwent liver biopsy. The study included 15 cases of SOS, 9 cases of inducement of gymura segetum, 2 cases of anti-rejection drugs, 1 case of chemotherapy drugs, 3 cases of Chinese herbal medicine: 7 male and 8 female with mean age 45 years old (range: 16-70 years). There were 33 cases of BCS: 19 males and 14 females with a mean age of 43 years (range: 18-64 years). Laboratory tests include: tumor markers, blood routine examination, liver function, total bilirubin, total protein, albumin, alkaline phosphatase, gamma-glutamyltransferase, proteinuria and coagulation function.

Imaging techniques

1. CT technique: The 31 patients were performed using 64-detector row CT scanners. The parameters were as follows: detector collimation, 0.625-1.25 mm; tube current, 380 mA; tube voltage, 120 KV; slice thickness, 5 mm; and pitch, 5 mm. Patients underwent a four-phase CT scan of the liver, including a noncontrast scan phase, a late arterial phase, a portal venous phase, and a delayed phase. An iodine contrast agent (370 mg I/ml (100 ml) was administered at a rate of 3 ml/s via a mechanical power injector (Medrad Stellant Dual Head Injector; Medrad, Warrendale, PA, USA) using a 20-gauge intravenous cannula placed in the antecubital vein. A smart prep contrast medium tracking technique was used during the arterial phase. When the CT value of the abdominal aorta reached or surpassed the threshold (150 HU), the scan was triggered. The venous phase was 65-70 s, and the delayed phase was 180-300 s. The thickness of the reconstructed image was 0.625 mm, and multiplanar reconstruction (MPR) was performed on the ADW 4.3 workstation. The latter two sets of spectral CT acquisitions were analyzed with GSI Viewer software 4.4 (GE Healthcare, Waukesha, Wisconsin) with a standard soft-tissue display window preset (WL 40 and WW 400).

2. MR technique**:** The 15 patients were performed with a 3.0T MR scanner (TIM TRIO; Siemens, Erlangen, Germany) using a 32-channel body coil. The protocol consisted of a 3-dimensional model voxel T1-

weighted (turbo-fast low angle shot (Turbo-FLASH), fast and small-angle excitation) breath-hold scanning sequence (TR/TE of 110.00 ms/2.46 ms, slice thickness and gap of 5/1.5 mm, matrix size of 320 × 154, and FOV of 440 mm × 640 mm), a T2-weighted (Turbo-FLASH, single excitation half Fourier collection fast spin-echo sequence) breath-hold scanning sequence (TR/TE of 1200 ms/88 ms, slice thickness and gap of 5/1.5 mm, matrix size of 384 × 200, and FOV of 616 mm × 768 mm), a diffusion-weighted imaging (DWI) scanning sequence (b-values of 0, 150 and 800 s/mm^2) with an echo-planar imaging (EPI) sequence, and a Gd-BOPTA dynamic enhanced scan (three-dimensional volume interpolation screen sequence (3D-VIBE) transection imaging). Gd-BOPTA was administered at a dosage of 0.2 mmol/kg at a rate of 2 mL per second followed by a 20-mL saline flush. After administering the contrast agent, early arterial phase (22 s), late arterial phase (44 s), portal venous phase (60 s), equilibrium phase (3-10 min), and additional hepatobiliary phase (1-2 hours) images were obtained.

Image analysis

Image analysis: 2 radiologists and 2 pathologists read the film together. If there is any difference, a consensus diagnosis should be reached through consultation. Data analysis included clinical symptoms, laboratory tests, and histopathological examinations. Image analysis included liver and gallbladder morphology, ascites, collateral circulation, liver enhancement, lesion scope and lesion distribution.

Pathological examination: The specimens were histopathologically examined by HE staining, followed by immunohistochemical examination. All pathological specimens were retrospectively analyzed by experienced pathologists.

Statistical analysis: The prevalence of test results was determined by the percentage of patients with abnormalities. All data were analyzed by SPSS 22.0 statistical software, measurement data were expressed as mean ± standard deviation (X±s), comparison of mean values between two groups was performed by T test, count data was expressed as number of cases (composition ratio), and comparison between groups was performed by Fisher test. $P<0.05$ was considered statistically significant.

Results

Clinical manifestation

The clinical data came from electronic medical record of our hospital. The age and gender composition and clinical symptoms of the two groups of patients are listed in Table 1. There was no statistically significant difference between the two groups except for right upper abdominal pain and weakness.

Table 1
Clinical manifestation of all included patients

Clinical manifestations	15 SOS (%)	33 BCS (%)	P
Sex			
Female	8 (53.3%)	14 (42.4%)	
Male	7 (46.7%)	19 (57.6%)	
Mean age	45	43	
Right upper pain	13(86.7%)	8(24.2%)	<0.01
Nausea,vomiting	1(6.7%)	2(6.1%)	0.938
Oliguria/anuria	2(13.3%)	2(6.1%)	0.409
Fatigue	7(46.7%)	4(12.1%)	<0.01

Laboratory examination Results

Statistical data of laboratory indicators of the two groups of patients are listed in Table 2. There were significant differences in total protein, albumin, Gamma-glutamyltransferase, alkaline phosphatase, and prothrombin time between the two groups. It also indicates that the liver function of SOS patients is more seriously impaired.

Table 2
Laboratory tests

laboratory tests	15 SOS (%)	33 BCS (%)	P
HGB (<110 g/L)	3 (20%)	7 (21.2%)	0.926
Blood platelet (<10×109/L)	1 (6.7%)	0	0.140
TBiL (>34.2 mmol/L)	15 (100%)	27 (81.2%)	0.080
DBiL (>6.8 mmol/L)	15 (100%)	27 (81.2%)	0.080
Total protein (<60 g/L)	10 (66.7%)	3 (9.1%)	<0.01
Albumin (<35 g/L)	10 (66.7%)	3 (9.1%)	<0.01
AKP (>135 U/L)	9 (60%)	2 (6.1%)	<0.01
γ-GT (>50 U/L)	15 (100%)	2 (6.1%)	<0.01
Prothrombin time (>14.5 s)	15 (100%)	7 (21.2%)	<0.01
Gamma-glutamyltransferase YGT, Alkaline phosphatase AKP, TBiL Total bilirubin, DBiL Direct bilirubin, Hemoglobin HGB			

Imaging findings

1. SOS imaging findings: twelve patients (80%) showed hepatomegaly, and 5 patients (33.3%) showed enlarged caudate lobe. MDCT and MR T1WI plain scan showed that the liver parenchyma showed diffuse or geographically hypoattenuation or hypointensity areas and patchy slightly hyperintensity on T2WI. Post-contrast MDCT and MR: hepatic artery and portal vein were clearly shown, heterogeneity patchy enhancement could be seen at portal vein phase and delayed phase in liver parenchyma, 12 cases (80%) were mainly distributed around hepatic main vein, and 3 cases (20%) presented diffuse distribution in liver (Fig. 1–4). Post-contrast, 13 cases (86.7%) showed non-enhanced areas lasting to the delay phase, only 2 cases (13.3%) tended to enhancement homogeneity. 12 cases (80%) showed hepatic vein narrowing or disappearance, and 2 cases (13.3%) showed widening of periportal space. Ten patients were followed up for 1 month to 3 years, 2 underwent liver transplantation, 5 patients improved, and 3 remained unchanged. Improved cases first appeared 1 months later onset, manifested in the enhanced area within the liver parenchyma is enlarged in the venous phase and delayed phase, and the development of hepatic main vein was thickening and clearer than before. MDCT and MR can well show the morphology, distribution and evolution process of abnormal enhancement in the liver.

2. BCS imaging findings: due to the obstruction of hepatic venous outflow, the 31 patients (80%) showed hepatomegaly, and 25 patients (75.8%) showed enlarged caudate lobe. The post-sinusoidal pressure was increased, the enhancement around the liver was weakened in the arterial phase, and the liver presented

hypoattenuation or hypointensity on CT or MRI. The portal vein phase showed a reversal pattern, with the contrast agent flowing out of the central region and enhancement weakening, while the surrounding region gradually enhancement with the accumulation of contrast agent. In the delayed phase, 30 cases (90.1%) showed homogeneity enhancement (Fig. 5–6). Due to separate venous drainage, caudate lobe enhancement was significant and enlarged (75.8%). Thrombi showed as intravascular filling defects on contrast-enhanced CT and MRI, hepatic venous thrombosis (42.4%), and inferior vena cava thrombosis (18.2%).

3. There were statistically significant differences between the two groups in caudate lobe enlargement, gallbladder wall thickening, ascites, collateral circulation, cloverleaf or claw-like enhancement around the main hepatic vein, and homogeneous enhancement in the delay period. Common imaging features were hepatic and splenic enlargement, periportal edema, and hepatic venous stenosis and dilatation. A list of these statistical results is provided in Table 3.

Table 3
Image findings

Imaging findings	15 SOS (%)	33 BCS (%)	P
Hepatomegaly	12 (80%)	31 (93.9%)	0.149
Caudate lobe enlargement	5 (33.3%)	25 (75.8%)	<0.01
Splenomegaly	12 (80%)	27 (81.8%)	0.884
Gallbladder wall thickening	10 (66.7%)	6 (18.2%)	<0.01
Ascites	12 (80%)	9 (27.3%)	<0.01
Collateral circulation	7 (46.7%)	31 (93.9%)	<0.01
Periportal edema	2 (13.3%)	1 (3.0%)	0.179
Hepatic vein stenosis	12 (80%)	7 (21.2%)	3.896
Hepatic vein dilatation	0	5 (15.2%)	0.116
Cloverleaf or claw-like shapes	12 (80%)	0	<0.01
Diffuse patchy enhancement	3 (20%)	31 (93.9%)	<0.01
Homogeneous in DH	2(13.3%)	30 (90.1%)	<0.01
Cloverleaf or claw-like shapes: enhancement around the main hepatic vein. DH: the delayed phase in CT or MR			

Liver biopsy pathology

SOS in the acute stage showed varying degrees of centrilobular sinusoidal congestion, dilatation, and hemorrhage with atrophy of the hepatocyte plate. The central veins showed intimal edema, endodermatitis and periphlebitis. In the later stage, it showed fibrosis or occlusion around the termimnal hepatic venules, collagen deposition occurred in the congested area, and hepatocytes proliferated around the portal area to form inverted hepatic lobules.

In the acute stage of BCS, sinusoidal dilatation and hemorrhage were seen, and hepatocyte atrophy and loss were marked around the terminal hepatic venules. In the chronic phase, fibrosis occurred around the blocking veins, the vascular contour was unclear. The hepatocytes proliferated in non venous occlusion area, and forming large regenerative nodules or pseudolobules.

Discussion

Sinusoidal obstruction syndrome (SOS), first reported by Jelliffe in 1954[10]. In 1957, Stein discovered that the pathological mechanism of SOS is hepatic venules occlusion process, namely the thickening of the vessel wall caused by endophlebitis. Unlike classic BCS, there is no thrombosis in the hepatic vein or inferior vena cava. This occlusion may be partial or complete due to a centripetal intimal filling of the vessel wall due to endophlebitis. Early on the intima is severely swollen with edema, but later connective tissue forms. Occlusion of the veins causes intense central lobular congestion, which widens the venous sinuses, ruptures and forms a blood lake. The pressure of the blood lake causes necrosis of the surrounding hepatocytes. Finally, compensatory fibrosis alters the structure of the liver and develops into a centrilobular cirrhosis. [11]. In recent years, it has been found that SOS damages the epithelial cells of sinusoids and hepatocytes in the 3 zones of hepatic acinus, and the shedding of endothelial cells leads to the occlusion of hepatic sinuses and terminal hepatic venules, while large hepatic veins were patent and there was a nonthrombotic occlusion of central and sublobular hepatic veins by subendothelial edema and fibrosis [12, 13]. In addition to endothelial cell shedding, blood flow obstruction is promoted by the proliferation of perisinusoidal stellate cells and subendothelial fibroblasts in the terminal hepatic vein followed by the deposition of the extracellular matrix. Then perivenular fibrosis spreads into the liver parenchyma [14]. Triggers include high-dose chemotherapy, Inflammation and cytokines released by transplantation, release of endotoxin, alloreactivity, calcineurin inhibitor and so on. In addition to the above triggers, SOS risk also depends on the genetic predisposition of the patient and that development of SOS may be rapid and unpredictable [15].

In Western countries, SOS is now recognised as a complication most commonly associated with high-dose chemotherapy and stem cell transplantation [16]. In recent years, more and more literature has been published on Gynura segetum induction of SOS, a kind of pyrrolizidine alkaloids containing herbal medicine widely used in China and some Asian countries [17, 18]. The parenchyma of this disease is blocked outflow from the sinusoidal and centrilobular vein, leading to liver congestion and enlargement, and is one of the three most common causes of death in bone marrow transplant patients. The current diagnosis is by reference to Seattle and Baltimore criteria and is based on clinical features including

painful hepatomegaly, hyperbilirubinemia and fluid retention [1, 6]. The reported mortality of SOS varies from 20 to 50%. While there is a gradual resolution of symptoms in mild and moderate patients, the mortality of severe patients approaches 100%, often involving multiple organ failure (MOF). The patients who develop hyperbilirubinaemia and significant fluid retention earlier and worsen faster are at high risk of severe SOS [18]. Clinical diagnosis needs to be rapid and accurate, because some patients will progress to MOF before diagnosis is clear, and the best opportunity for intervention will be lost. Although liver biopsy is the gold standard for diagnosis, it is often limited by thrombocytopenia, abnormal coagulation function and massive ascites [19]. In addition, the heterogeneity distribution of lesions also affects the accuracy of biopsy [6]. The decrease rate of total protein and albumin in SOS patients was higher than that of BCS, indicating that SOS patients suffered more serious liver function damage.

Liu et al. observed that different pathological features upon different stages by animal models of PAs-induced HSOS. In acute stage, sinusoidal congestion and dilation, the hepatocyte necrosis and the extravasation of erythrocytes in zone 3. In addition, macrophages infiltrated into the space of Disse, and engulfed erythrocytes. In sub-acute stage, pathologic examination showed complete loss of pericentral hepatocytes, sinusoidal dilatation, deposition of pigment granules [18]. The varieties of pathological manifestations depend on age, the PAs dose, the period, and individual variation [19]. BCS and congestive liver disease can also show sinusoidal congestion and hepatocyte necrosis, which are sometimes difficult to distinguish from histologically [6]. Imaging techniques have experienced major progress since the 1980s and the initial definition of the criteria for diagnosis of SOS/VOD, raising the possibility that they may contribute to refining such diagnosis today [1]. CT and MRI showed hepatomegaly, ascites, hepatic vein narrowing, gallbladder wall thickening, periportal edema, patchy signal enhancement of the liver. Zhou et al. reported that liver parenchyma surrounding the main hepatic veins demonstrated relatively normal enhancement compared to the rest of the patchy enhanced area of liver. This interesting finding is called "clover sign", suggest that the venules adjacent to the hepatic main vein are more likely to keep patent; the extent of abnormal patchy liver enhancement reflect the severity of the disease [20–24]. In present study, the SOS images showed that the enhancement distribution around the main hepatic vein was obvious, while the patchy enhancement was dominant in the BCS patients, which was related to the different pathogenesis, location and degree of liver parenchymal injury of the two diseases.

In practice, SOS is not only be distinguished from other rare cases of diffuse liver diseases, such as amyloidosis, glycogen storage disease, Wilson's disease and α-1antitrypsin deficiency, but also from the relatively rare BCS. BCS is a group of diseases characterized by partial or total hepatic veins outflow obstruction, with elevated sinusoidal pressure, portal hypertension, liver congestion, eventually hepatic fibrosis and cirrhosis [25, 26]. The clinical manifestation depends on the degree of venous obstruction and the patency of Intra- and extrahepatic collaterals. One quarter of patients have no underlying disease [27, 28]. Imaging findings included occlusion or compression of hepatic veins and/or inferior vena cava, formation of collateral circulation, caudate lobe enlargement, and delayed enhanced nodules formation [29]. This study showed that there was a statistical difference between the two diseases in the Intra- and

extrahepatic collaterals circulation, hepatic venous obstruction, parenchyma enhancement pattern, delayed phase enhances uniformity, and SOS caused more serious liver damage. In addition, SOS showed heterogeneous enhancement in the delayed phase of enhanced CT and/or MR, this is caused by sinusoidal or hepatic venule obstruction that is not or poorly enhanced. This kind of imaging manifestation also conforms to the pathological mechanism of the two diseases and can be used as one of the important imaging differentiation point of the two diseases.

It is difficult to obtain timely and reliable diagnosis by using the current clinical diagnostic criteria. Noninvasive imaging is becoming more and more important in SOS diagnosis and differential diagnosis. Combined with liver hemodynamic changes, liver parenchymal heterogeneity, damaged hepatocyte function, and portal hypertension imaging features provide important information for the identification of these diseases. The limitation of this study is that there are few subjects. Secondly, some patients presented thrombocytopenia and coagulation abnormalities and massive ascites, so histological evidence could not be obtained, which also limited the inclusion of more cases.

Declarations

Ethics approval and consent to participate

This retrospective research was approved by the Ethics Committee of Beijing Youan Hospital, Capital Medical University (No. 2019008; Beijing, China) in accordance with the Declaration of Helsinki, and the informed consent was waived by Ethics Committee of Beijing Youan Hospital, Capital Medical University.

Consent for publication

Not applicable.

Availability of data and materials

The datasets used and analyzed in this study are available from the corresponding author on reasonable request.

Competing interests

The authors declare that they have no competing interests. The funders had no role in the design of the study; in the collection, analyses, or interpretation of data; in the writing of the manuscript, or in the decision to publish the results.

Funding

This research was funded by National Natural Science Foundation of China (No. 81771806, 61936013); Project of Incubating Young and Middle-aged Talents (No. YNKTTS20180130).

Authors' contributions

Conceptualization, C. J.; methodology, C. J, D. Z.; software, C. J, D. Z. and H. L.; validation, C. J., D. Z. and H. L.; investigation, C. J. and R. L.; resources, J. F. and X. W., D. Z. and H. L.; data curation, C. J. and D. Z.; writing—original draft preparation, C. J.; writing—review and editing, C. J., D. Z. and H. L.; supervision, D. Z. and H. L.; funding acquisition, C. J. and H. L. All authors have read and agreed to the published version of the manuscript.

Acknowledgements

Not applicable.

Authors' information

[1] Department of Radiology, Beijing YouAn Hospital, Capital Medical University, Beijing, 100069, China; [2] Department of Pathology, Beijing YouAn Hospital, Capital Medical University, Beijing, 100069, China

References

1. Mohty M, Malard F, Abecassis M, et al. Revised diagnosis and severity criteria for sinusoidal obstruction syndrome/veno-occlusive disease in adult patients: a new classification from the European Society for Blood and Marrow Transplantation. Bone Marrow Transplant. 2016;51(7):906–912. PMID: 27183098; PMCID: PMC4935979.
2. Coppell JA, Richardson PG, Soiffer R, Martin PL, Kernan NA, Chen A, et al. Hepatic veno-occlusive disease following stem cell transplantation: incidence, clinical course, and outcome. Biol Blood Marrow Transplant. 2010;16:157–168. PMID: 20626434; PMCID: PMC6493817.
3. Lin G, Wang JY, Li N, et al. Hepatic sinusoidal obstruction syndrome associated with consumption of Gynura segetum. J Hepatol. 2011;54(4):666–673. PMID: 21146894.
4. Gao H, Li N, Wang JY, Zhang SC, Lin G. Definitive diagnosis of hepatic sinusoidal obstruction syndrome induced by pyrrolizidine alkaloids. J Dig Dis. 2012;13(1):33-39. PMID: 22188914.
5. Wang JY, Gao H. Tusanqi and hepatic sinusoidal obstruction syndrome. J Dig Dis. 2014;15(3):105-107. PMID: 24528632.
6. Kan X, Ye J, Rong X, Lu Z, Li X, Wang Y, Yang L, Xu K, Song Y, Hou X. Diagnostic performance of Contrast-enhanced CT in Pyrrolizidine Alkaloids-induced Hepatic Sinusoidal Obstructive Syndrome. Sci Rep. 2016 Nov 29;6:37998. PMID: 27897243; PMCID: PMC5126558.
7. Yoneda N, Matsui O, Ikeno H, et al. Correlation between Gd-EOB-DTPA-enhanced MR imaging findings and OATP1B3 expression in chemotherapy-associated sinusoidal obstruction syndrome. Abdom Imaging. 2015;40(8):3099–3103. PMID: 26187715.
8. Vernuccio F, Dioguardi Burgio M, Barbiera F, et al. CT and MR imaging of chemotherapy-induced hepatopathy. Abdom Radiol (NY). 2019;44(10):3312-3324. PMID: 31435760.
9. Guo T, Li X, Yang X, et al. Gadoxetic Acid-Enhanced Hepatobiliary-Phase Magnetic Resonance Imaging for Pyrrolizidine Alkaloid-Induced Hepatic Sinusoidal Obstruction Syndrome and

Association with Liver Function. Sci Rep. 2019;9(1):1231. PMID: 30718698; PMCID: PMC6362127.

10. JELLIFFE DB, BRAS G, STUART KL. Veno-occlusive disease of the liver. Pediatrics. 1954 Oct;14(4):334–9. PMID: 13204101.
11. STEIN H. Veno-occlusive disease of liver in African children. Br Med J. 1957 Jun 29;1(5034):1496-9. PMID: 13436832.
12. Valla DC, Cazals-Hatem D. Sinusoidal obstruction syndrome. Clin Res Hepatol Gastroenterol. 2016 Sep;40(4):378–85. PMID: 27038846.
13. Fan CQ, Crawford JM. Sinusoidal obstruction syndrome (hepatic veno-occlusive disease). J Clin Exp Hepatol. 2014 Dec;4(4):332–46. PMID: 25755580.
14. Bonifazi F, Barbato F, Ravaioli F, Sessa M, Defrancesco I, Arpinati M, Cavo M, Colecchia A. Diagnosis and Treatment of VOD/SOS After Allogeneic Hematopoietic Stem Cell Transplantation. Front Immunol. 2020 Apr 3;11:489. PMID: 32318059; PMCID: PMC7147118.
15. Corbacioglu S, Carreras E, Ansari M, Balduzzi A, Cesaro S, Dalle JH, Dignan F, Gibson B, Guengoer T, Gruhn B, Lankester A, Locatelli F, Pagliuca A, Peters C, Richardson PG, Schulz AS, Sedlacek P, Stein J, Sykora KW, Toporski J, Trigoso E, Vetteranta K, Wachowiak J, Wallhult E, Wynn R, Yaniv I, Yesilipek A, Mohty M, Bader P. Diagnosis and severity criteria for sinusoidal obstruction syndrome/veno-occlusive disease in pediatric patients: a new classification from the European society for blood and marrow transplantation. Bone Marrow Transplant. 2018 Feb;53(2):138–145. PMID: 28759025; PMCID: PMC5803572.
16. Kami M, Mori S, Tanikawa S, Akiyama H, Onozawa Y, Tanaka T, Okamoto R, Maeda Y, Sasaki T, Kaku H, Matsuura Y, Hiruma K, Sakamaki H. Risk factors for hepatic veno-occlusive disease after bone marrow transplantation: retrospective analysis of 137 cases at a single institution. Bone Marrow Transplant. 1997 Sep;20(5):397–402. PMID: 9339756.
17. Lin G, Tang J, Liu XQ, Jiang Y, Zheng J. Deacetylclivorine: a gender-selective metabolite of clivorine formed in female Sprague-Dawley rat liver microsomes. Drug Metab Dispos. 2007;35(4):607–613. PMID: 17237157.
18. Liu F, Rong X, Guo H, Xu D, Liu C, Meng L, Yang X, Guo T, Kan X, Song Y. Clinical characteristics, CT signs, and pathological findings of Pyrrolizidine alkaloids-induced sinusoidal obstructive syndrome: a retrospective study. BMC Gastroenterol. 2020 Feb 4;20(1):30. PMID: 32019495
19. Chen Z, Huo JR. Hepatic veno-occlusive disease associated with toxicity of pyrrolizidine alkaloids in herbal preparations. Neth J Med. 2010;68(6):252-260. PMID: 20558855.
20. Erturk SM, Mortelé KJ, Binkert CA, et al. CT features of hepatic venoocclusive disease and hepatic graft-versus-host disease in patients after hematopoietic stem cell transplantation. AJR Am J Roentgenol. 2006;186(6):1497–1501. PMID: 16714636.
21. Han NY, Park BJ, Kim MJ, Sung DJ, Cho SB. Hepatic Parenchymal Heterogeneity on Contrast-enhanced CT Scans Following Oxaliplatin-based Chemotherapy: Natural History and Association with Clinical Evidence of Sinusoidal Obstruction Syndrome. Radiology. 2015;276(3):766–774. PMID: 25822471.

22. Cayet S, Pasco J, Dujardin F, et al. Diagnostic performance of contrast-enhanced CT-scan in sinusoidal obstruction syndrome induced by chemotherapy of colorectal liver metastases: Radio-pathological correlation. Eur J Radiol. 2017;94:180–190. PMID: 28712693.
23. Zhou H, Wang YX, Lou HY, Xu XJ, Zhang MM. Hepatic sinusoidal obstruction syndrome caused by herbal medicine: CT and MRI features. Korean J Radiol. 2014 Mar-Apr;15(2):218–25. PMID: 24643319; PMCID: PMC3955788.
24. Wang C, Wu X, Xie W, Ren X, Zhang W, Xu J. Quantitative Analysis of CT Images in Patients with Pyrrolizidine Alkaloid-Induced Sinusoidal Obstruction Syndrome. Sci Rep. 2019;9(1):2179. PMID: 30778132; PMCID: PMC6379399.
25. Vernuccio F, Dioguardi Burgio M, Barbiera F, et al. CT and MR imaging of chemotherapy-induced hepatopathy. Abdom Radiol (NY). 2019;44(10):3312-3324. PMID: 31435760.
26. Bansal V, Gupta P, Sinha S, et al. Budd-Chiari syndrome: imaging review. Br J Radiol. 2018;91(1092):20180441. PMID: 30004805; PMCID: PMC6319835.
27. Aydinli M, Bayraktar Y. Budd-Chiari syndrome: etiology, pathogenesis and diagnosis. World J Gastroenterol. 2007;13(19):2693–2696. PMID: 17569137; PMCID: PMC4147117.
28. Noone TC, Semelka RC, Siegelman ES, Balci NC, Hussain SM, Kim PN, Mitchell DG. Budd-Chiari syndrome: spectrum of appearances of acute, subacute, and chronic disease with magnetic resonance imaging. J Magn Reson Imaging. 2000 Jan;11(1):44–50. PMID: 10676619.
29. Van Wettere M, Bruno O, Rautou PE, Vilgrain V, Ronot M. Diagnosis of Budd-Chiari syndrome. Abdom Radiol (NY). 2018 Aug;43(8):1896–1907. PMID: 29285598.

Figures

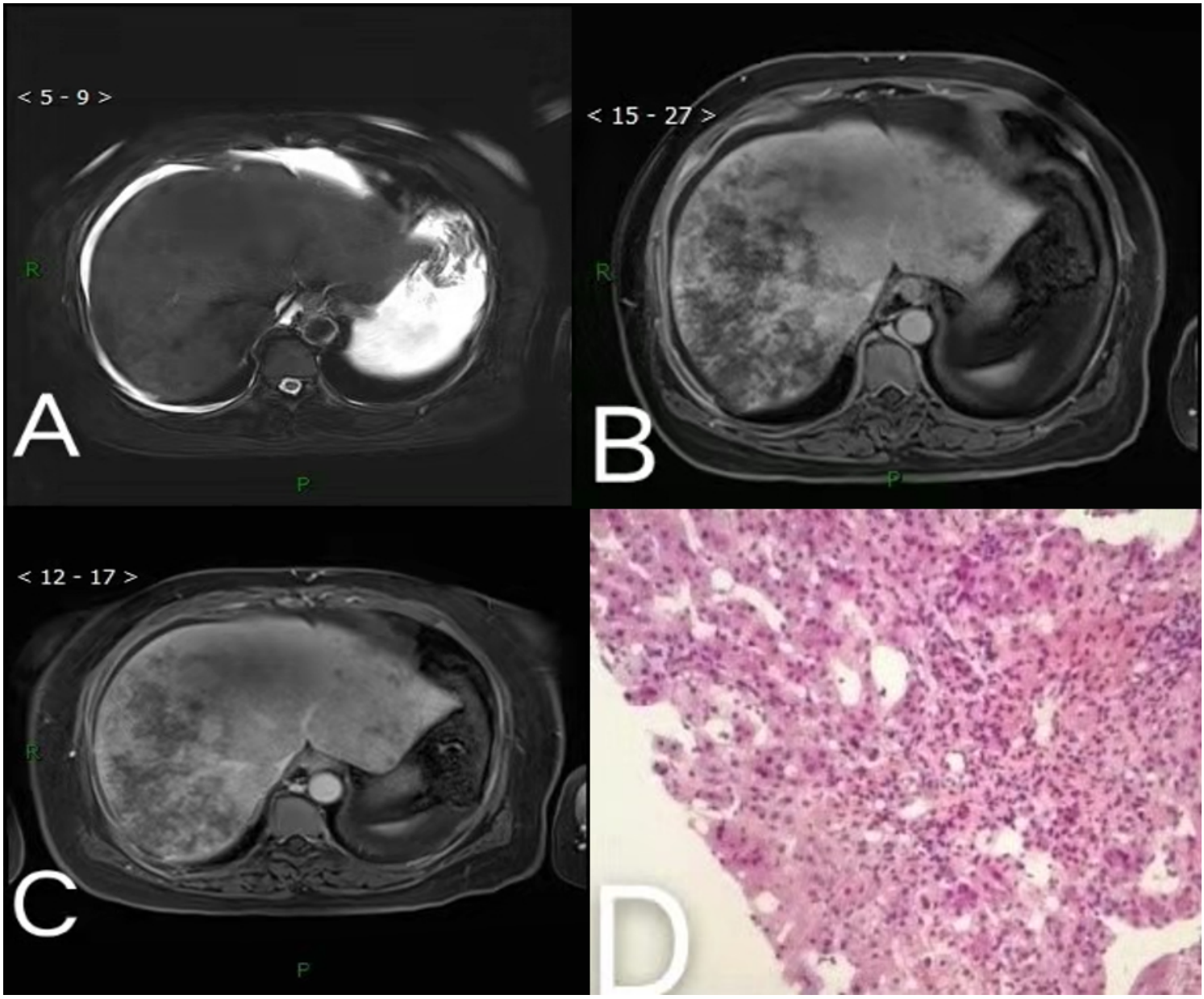

Figure 1

53-year-old woman diagnosed with hepatic sinusoidal obstruction syndrome eight months after ingestion of Gynura segetum. A. Diffuse patchy slightly hyperintensity are demonstrated on fat-suppressed T2-weighted MRI. B. Contrast-enhanced MRI equilibrium phases scan demonstrates diffuse heterogeneity patchy liver enhancement with prominent distribution around hepatic veins, hepatic vein narrowingor vague (arrows). C. A month later, contrast-enhanced MRI scan shows that patchy enhanced area is enlarged in the venous phase and delayed phase, and hepatic vein was thickening and clearer than before (arrows). D. The hematoxylineosin (HE) staining at ×200 magnification shows expansion and congestion around the central hepatic vein and hepatic sinus, hepatocyte edema, and mild central venous fibrosis.

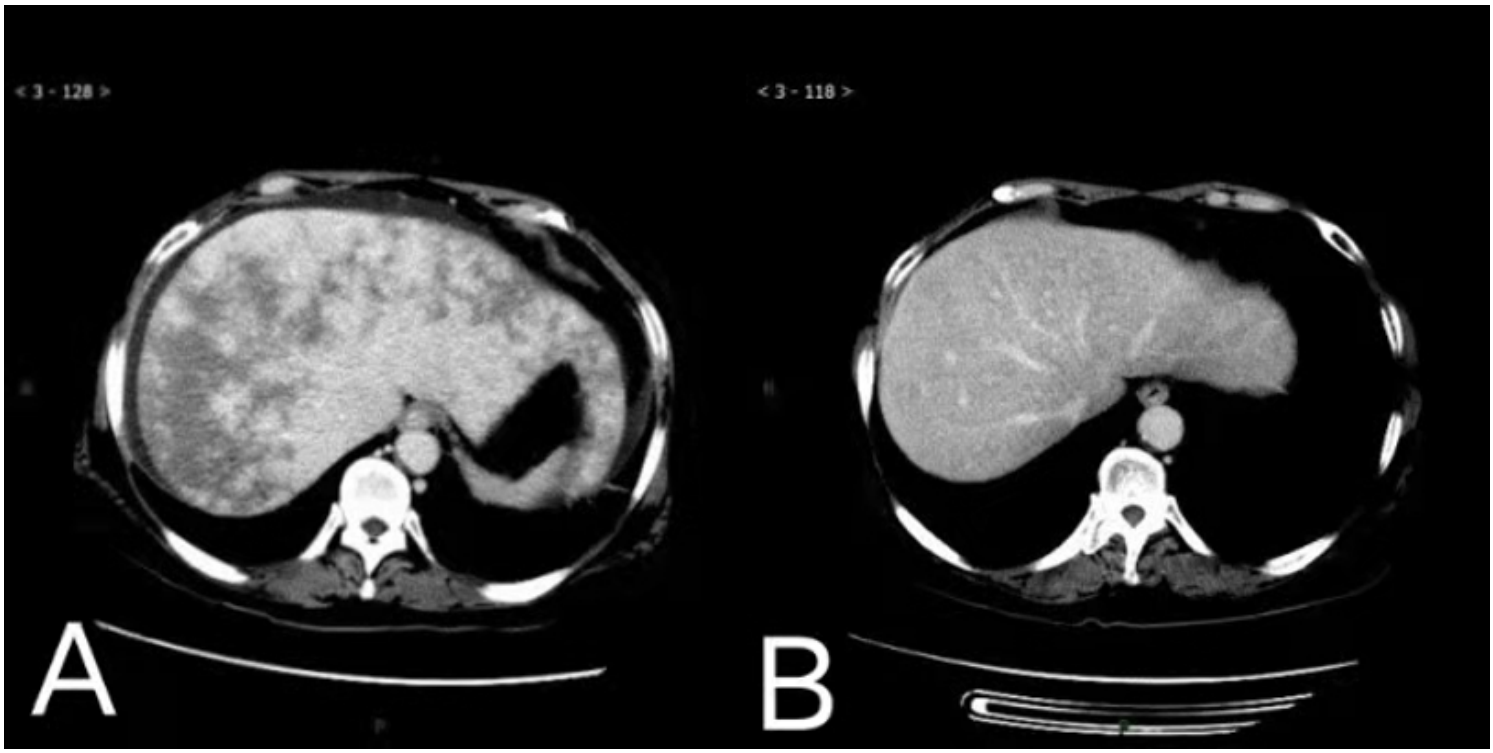

Figure 2

59-year-old man diagnosed with hepatic sinusoidal obstruction syndrome six months after ingestion of Chinese herb. A. Contrast-enhanced delayed phase CT scans show diffuse patchy enhancement and claw-like distribution around hepatic veins, the left lobe of the liver is significantly enlarged and ascites. B. Three months later, contrast-enhanced CT scan shows that liver uniform enhancement and the hepatic veins showed clearly. The left lobe of the liver shrinks and ascites subsided.

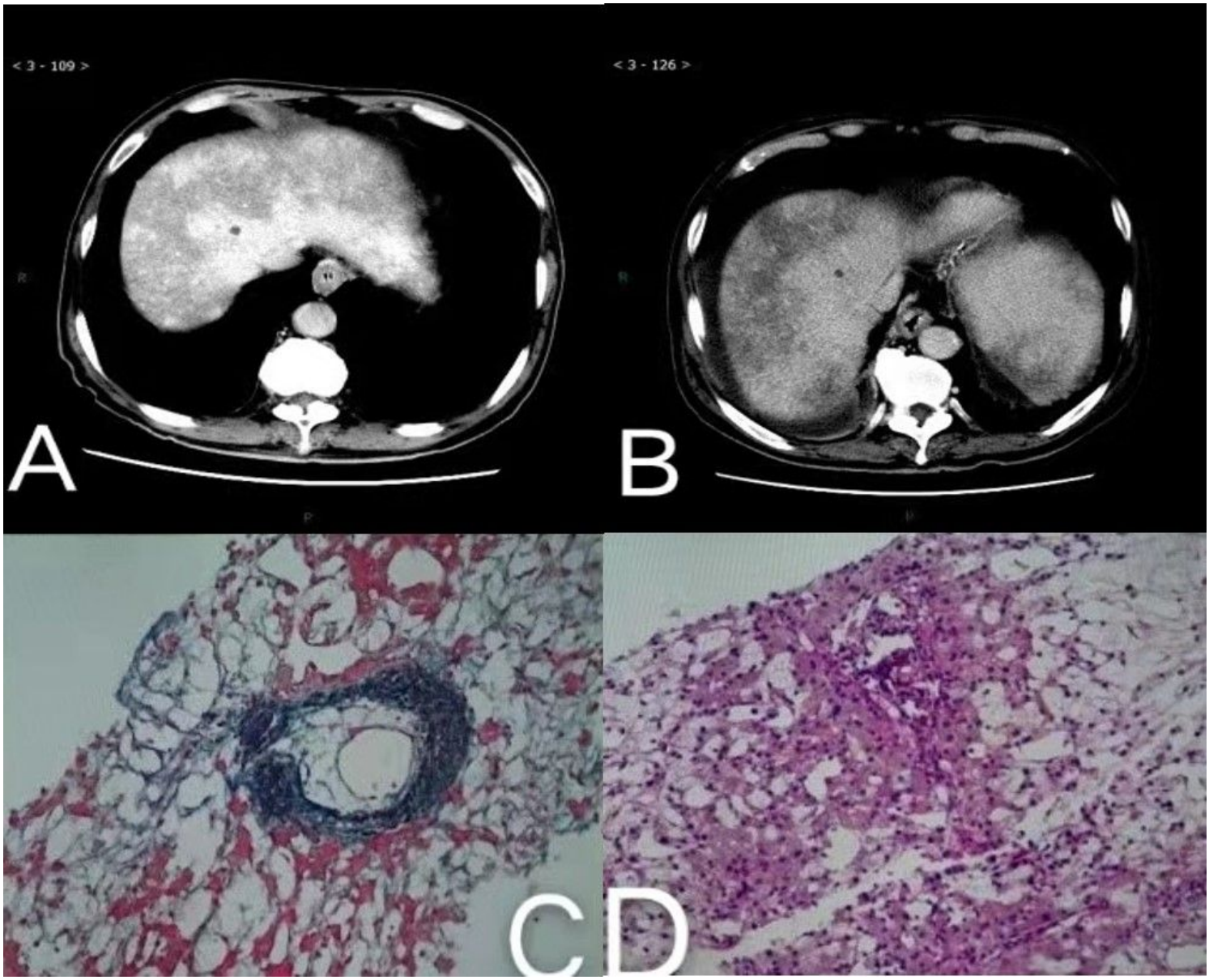

Figure 3

62-year-old man diagnosed with hepatic sinusoidal obstruction syndrome a months after ingestion of Gynura segetum. A. Contrast-enhanced delayed phase CT scans demonstrate clover-like enhancement surrounding hepatic veins. B. Seven weeks later, contrast-enhanced CT scan shows that patchy enhanced area is enlarged in the portal phase and delayed phase than before. C. Masson staining at ×200 magnification shows the thickening of the inner vein or hepatic vein, and endovascular stenosis. D. The hematoxylineosin (HE) staining at ×200 magnification shows hepatic sinus expansion and congestion with atrophy of the hepatocyte plate.

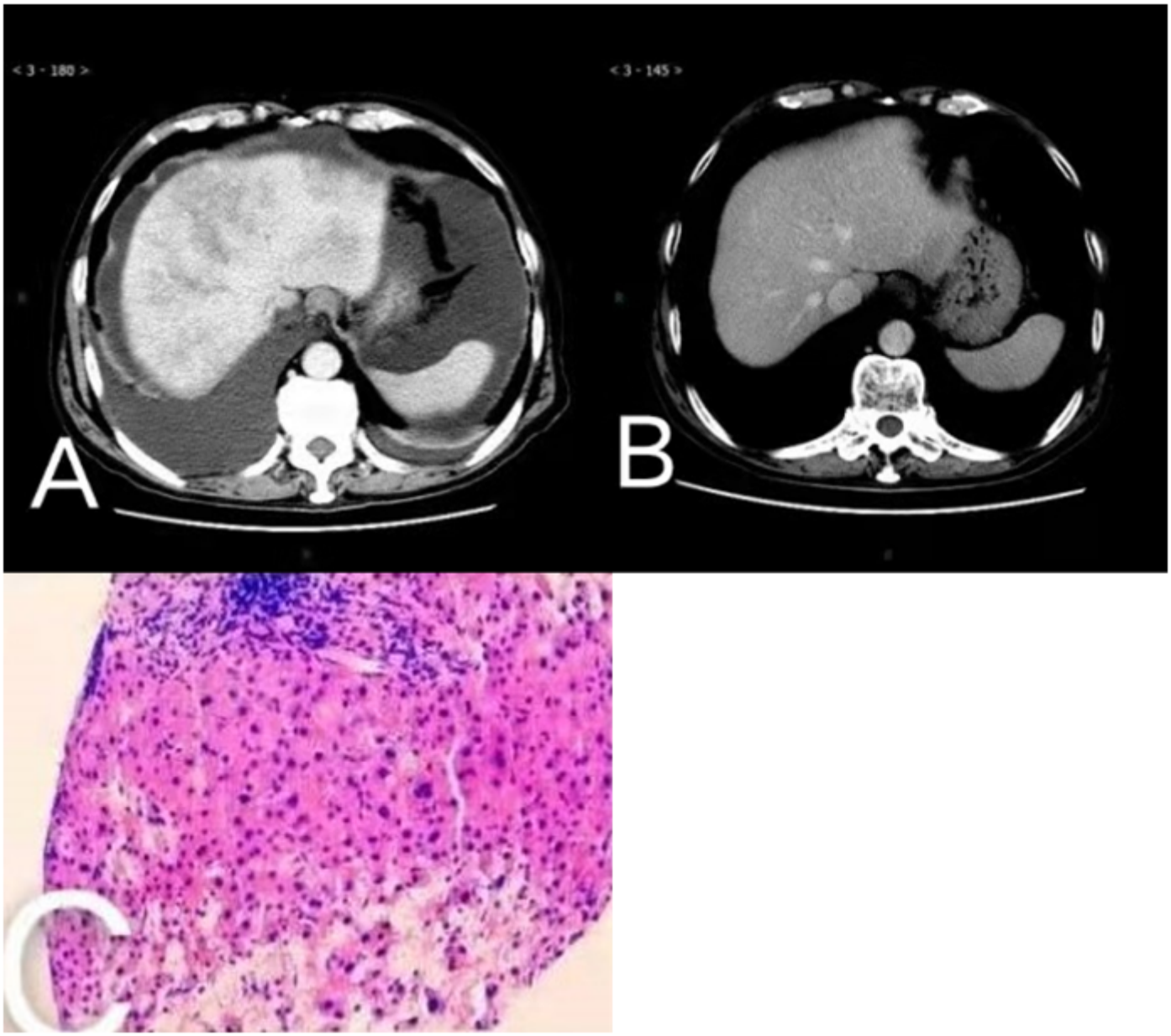

Figure 4

62-year-old man diagnosed with hepatic sinusoidal obstruction syndrome a months after ingestion of Chinese herb for psoriasis. A. Delayed phase contrast-enhanced CT scans demonstrate clover-like enhancement surrounding hepatic veins, massive ascites and pleural effusion. B. Three months later, contrast-enhanced CT scan shows that liver uniform enhancement and the hepatic veins showed clearly, ascites and pleural effusion subsided. C. The hematoxylineosin (HE) staining at ×200 magnification shows expansion and congestion around the central hepatic vein and hepatic sinus with atrophy of the hepatocyte plate.

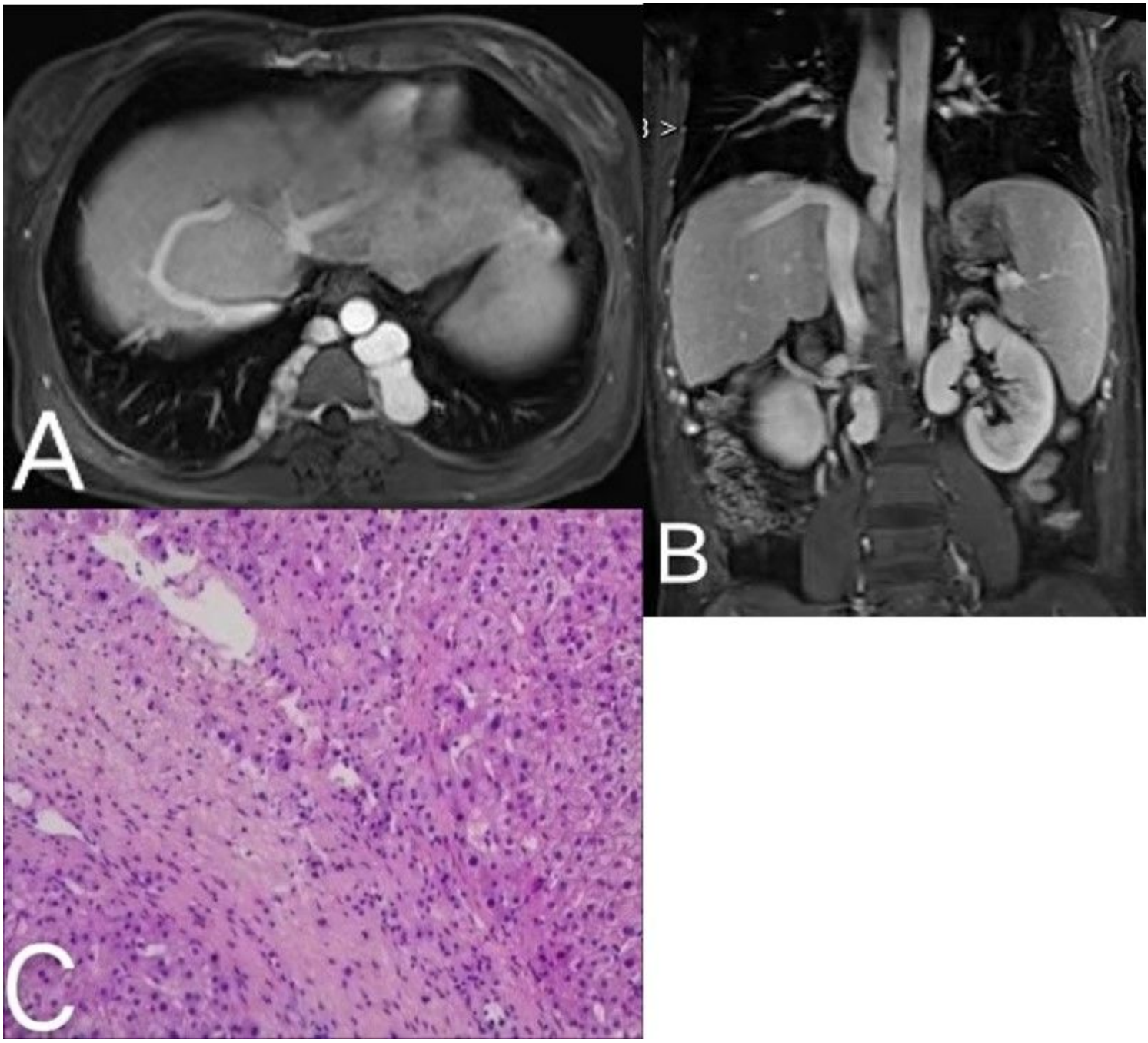

Figure 5

37-years-woman was admitted for hepatosplenomegaly. A. Contrast-enhanced MRI equilibrium phase shows liver uniform enhancement, intrahepatic veno-venous collateral between the hepatic veins with conspicuous collateral veins. B. Contrast-enhanced MRI portal phase shows obstruction of the IVC. C. The hematoxylineosin (HE) staining at×200 magnification shows expansion central hepatic vein and hepatic sinus with atrophy of the hepatocyte plate.

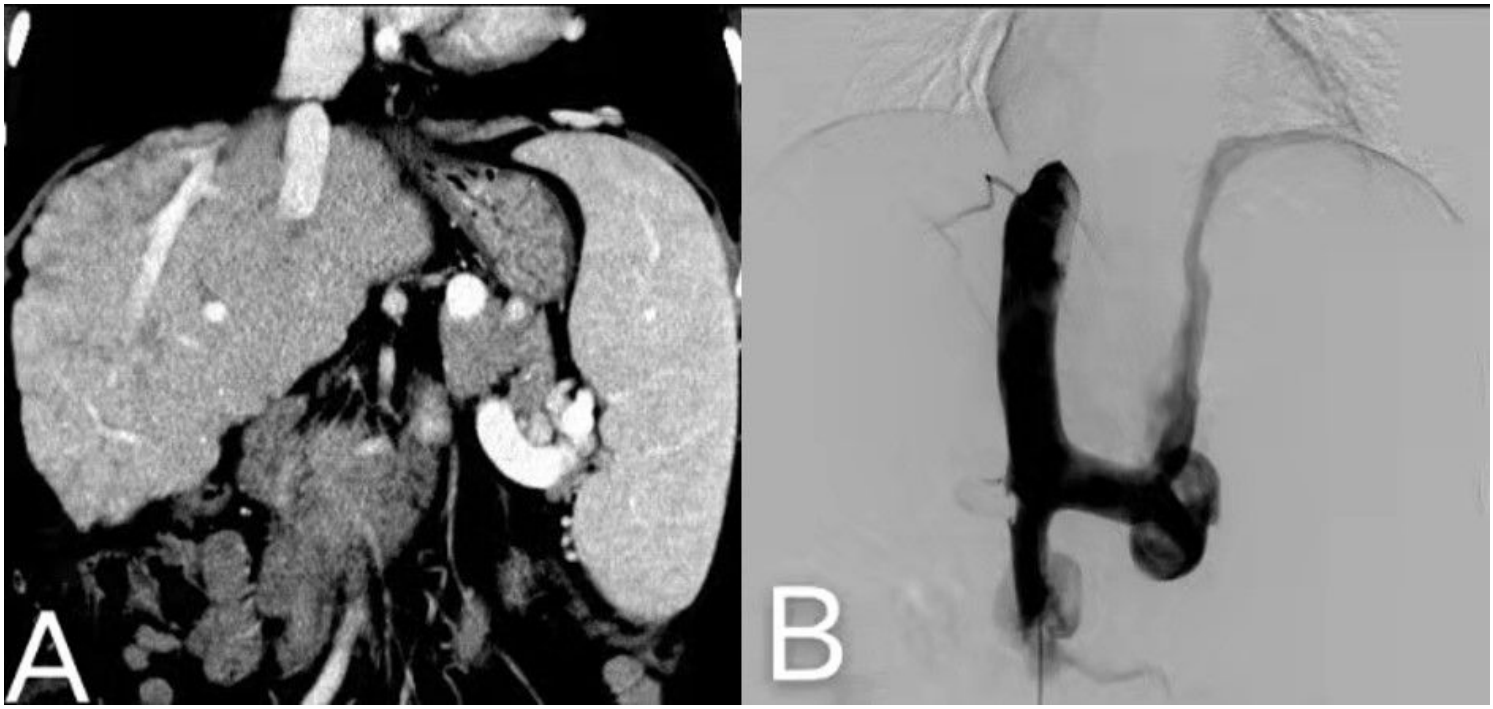

Figure 6

42-years-woman was admitted for hepatosplenomegaly. A. Contrast-enhanced CT portal phase shows liver uniform enhancement with obstruction of the IVC. B. DSA showed no development was seen in the superior hepatic segment of inferior vena cava.